*JGR, Solid Earth*

Supporting Information for

# The Signature and Elimination of Sediment Reverberations on Submarine Receiver Functions

**Ziqi Zhang[1*]**, and Tolulope Olugboji[1]

[1] *Department of Earth and Environmental Sciences, University of Rochester, NY*

## Contents of this file

Text S1, S2; Figures S1, S2; Table S1.

## Introduction

We provide supporting information showing extended analysis: Text S1 shows how we derive the amplitudes and polarities of different phases in the receiver functions using reflection and transmission coefficients; Text S2 shows how we adjust the traveltimes in the $\kappa - v_p - H$ stacks when sediment presents; Figure S1 and Figure S2 show the mean power spectra and coherence on vertical and radial components at each station, respectively; Table S1 shows detailed information of each station.

**Text S1**

**Text S1-A: Reflection and Transmission Coefficient Matrices**

Seismic reflection and transmission coefficients depend on the seismic wave velocities and densities on either side of the boundary and on the incident wave horizontal slowness, or ray parameter. The coefficients are given by (Aki and Richards 2002; Lay and Wallace 1995):

$$R_{pp} = [(b\eta_{\alpha_1} - c\eta_{\alpha_2})F - (a + d\eta_{\alpha_1}\eta_{\beta_2})Hp^2]/D$$

$$R_{ps} = -2[\eta_{\alpha_1}(ab + cd\eta_{\alpha_2}\eta_{\beta_2})p(\alpha_1/\beta_1)]/D$$

$$R_{ss} = -[(b\eta_{\beta_1} - c\eta_{\beta_2})E - (a + b\eta_{\alpha_2}\eta_{\beta_1})Gp^2]/D$$

$$R_{sp} = -[2\eta_{\beta_1}(ab + cd\eta_{\alpha_2}\eta_{\beta_2})p(\beta_1/\alpha_1)]/D$$

$$T_{pp} = [2\rho_1\eta_{\alpha_1}F(\alpha_1/\alpha_2)]/D$$

$$T_{ps} = [2\rho_1\eta_{\alpha_1}Hp(\alpha_1/\beta_2)]/D$$

$$T_{ss} = [2\rho_1\eta_{\beta_1}E(\alpha_2/\beta_2)]/D$$

$$T_{sp} = -[2\rho_1\eta_{\beta_1}Gp(\alpha_2/\beta_1)]/D$$

where

$$a = \rho_2(1 - 2\beta_2^2p^2) - \rho_1(1 - 2\beta_1^2p^2)$$

$$b = \rho_2(1 - 2\beta_2^2p^2) + 2\rho_1\beta_1^2p^2$$

$$c = \rho_1(1 - 2\beta_1^2p^2) + 2\rho_2\beta_2^2p^2$$

$$d = 2(\rho_2\beta_2^2 - \rho_1\beta_1^2)$$

$$E = b\eta_{\alpha_1} + c\eta_{\alpha_2}$$

$$F = b\eta_{\beta_1} + c\eta_{\beta_2}$$

$$G = a - d\eta_{\alpha_1}\eta_{\beta_2}$$

$$H = a - d\eta_{\alpha_2}\eta_{\beta_1}$$

$$D = EF + GHp^2$$

**Text S1-B: Amplitude and Polarity of Phases in Ocean Models**

Assuming unit amplitude of incoming teleseismic P wave beneath the LAB:

For model M1, the amplitude and polarity of each phase is given by:

$$P_mS = T_1^{PP}T_2^{PP}$$

$$PP_mS = \left(\prod_{i=1}^{2} T_i^{PP}\right)\mathbf{R}_3^{PP}R_2^{PS}$$

$$PS_mS = \left(\prod_{i=1}^{2} T_i^{PP}\right)\mathbf{R}_3^{PS}R_2^{SS}$$

$$P_lS = T_1^{PS}T_2^{SS}$$

$$PP_lS = \left(\prod_{i=1}^{2} T_i^{PP}\right)R_3^{PP}\mathbf{T}_2^{PP}\mathbf{R}_1^{PS}T_2^{SS}$$

$$PS_lS = \left(\prod_{i=1}^{2} T_i^{PP}\right)R_3^{PS}\mathbf{T}_2^{SS}\mathbf{R}_1^{SS}T_2^{SS}$$

using the reflection and transmission coefficients for each layer given in Text S1-A. Note that 1, 2 and 3 in the subscript of T and R indicate transmission and reflection coefficients on top of the asthenosphere, uppermost mantle and crust, respectively.

For model M2:

$$P_mS = T_1^{PP}T_2^{PS}T_3^{SS}$$

$$PP_mS = \left(\prod_{i=1}^{3} T_i^{PP}\right)R_4^{PP}\mathbf{T}_3^{PP}\mathbf{R}_2^{PS}T_3^{SS}$$

$$PS_mS = \left(\prod_{i=1}^{3} T_i^{PP}\right)R_4^{PS}\mathbf{T}_3^{SS}\mathbf{R}_2^{SS}T_3^{SS}$$

$$P_lS = T_1^{PS}T_2^{SS}T_3^{SS}$$

$$PP_lS = \left(\prod_{i=1}^{3} T_i^{PP}\right)R_4^{PP}\left(\prod_{i=2}^{3} \mathbf{T}_i^{PP}\right)R_1^{PS}\left(\prod_{i=2}^{3} T_i^{SS}\right)$$

$$PS_lS = \left(\prod_{i=1}^{3} T_i^{PP}\right) R_4^{PS} \left(\prod_{i=2}^{3} \mathbf{T}_i^{SS}\right) R_1^{SS} \left(\prod_{i=2}^{3} T_i^{SS}\right)$$

Note that 1, 2, 3 and 4 in the subscript of T and R indicate transmission and reflection coefficients on top of the asthenosphere, uppermost mantle, crust and sediment, respectively.

all bold-font reflection and transmission coefficients ($\mathbf{R}, \mathbf{T}$) indicate downgoing incidence ($\mathbf{R}^{PS}, \mathbf{T}^{SS} = \mathbf{R}^{\grave{S}\acute{P}}, \mathbf{T}^{\grave{S}\grave{S}}$), otherwise upgoing ($R^{SS}, T^{SS} = R^{\acute{S}\grave{S}}, T^{\acute{S}\acute{S}}$).

**Text S2: Time Correction in the Presence of Sediments**

Due to the delay effects of the sedimentary layer, the stacking and linear search technique described in section 2.x would fail if time delays associated with the sedimentary layer are not corrected for (Yeck, Sheehan, and Schulte-Pelkum 2013). Following (Yu et al. 2015), we adjust equation (6)-(7) to accommodate for the time delays:

$$\widetilde{t'}_{PmS}(p_i) = t'_{PmS}(p_i) + \delta t(p_i) \tag{S1a}$$

$$\widetilde{t'}_{PPmS}(p_i) = t'_{PPmS}(p_i) + \Delta t(p_i) - \delta t(p_i) \tag{S1b}$$

$$\widetilde{t'}_{PSmS}(p_i) = t'_{PPmS}(p_i) + \Delta t(p_i) + \delta t(p_i) \tag{S1c}$$

$$\widetilde{t}_{PPmS}(p_i) = \frac{A+B}{A-B}\left(t_{PmS}(p_i) - \delta t\right) + \Delta t(p_i) - \delta t(p_i) \tag{S2a}$$

$$\widetilde{t}_{PSmS}(p_i) = \frac{2A}{A-B}\left(t_{PmS}(p_i) - \delta t\right) + \Delta t(p_i) \tag{S2b}$$

where $\Delta t(p_i)$ and $\delta t(p_i)$ is the two-way travel time of the reverberations in the sediment and the time delay (relative to the direct P) of the *PbS* phase (Ps conversion from the bottom of sediment), respectively:

$$\Delta t(p_i) = \frac{2H_{sed}}{v_{s_{sed}}}\sqrt{1 - v_{s_{sed}}^2 p_i^2} \tag{S3a}$$

$$\delta t(p_i) = \frac{H_{sed}}{v_{s_{sed}}}\sqrt{1 - v_{s_{sed}}^2 p_i^2} - \frac{H_{sed}}{v_{p_{sed}}}\sqrt{1 - v_{p_{sed}}^2 p_i^2} \tag{S3b}$$

After the correction for the travel times associated with sediment, the station is virtually downward projected to the bottom of the sedimentary layer. The aforementioned stacking for $\kappa$ and $v_p$ and the linear search for $H$ can then be implemented to determine the sub-sediment crustal structure.

For the linear search for the thickness of Moho to LAB, we simply modify equation (9) by substituting the Moho-associated travel times by the time-corrected ones defined in equation (S1a)-(S1c):

$$t'_1 = \widetilde{t}_{P_lS}(p_i) = \hat{\widetilde{t'}}_{P_mS}(p_i) + \frac{H_{LAB}}{\hat{v}_{p_m}}(\hat{A}_m - \hat{B}_m) \tag{S4a}$$

$$t'_2 = \widetilde{t}_{PP_lS}(p_i) = \hat{\widetilde{t'}}_{P_mS}(p_i) + \frac{H_{LAB}}{\hat{v}_{p_m}}(\hat{A}_m + \hat{B}_m) \tag{S4b}$$

Then $H_{LAB}$ can be determined using the linear search defined in equation (8).

**Figure S1**

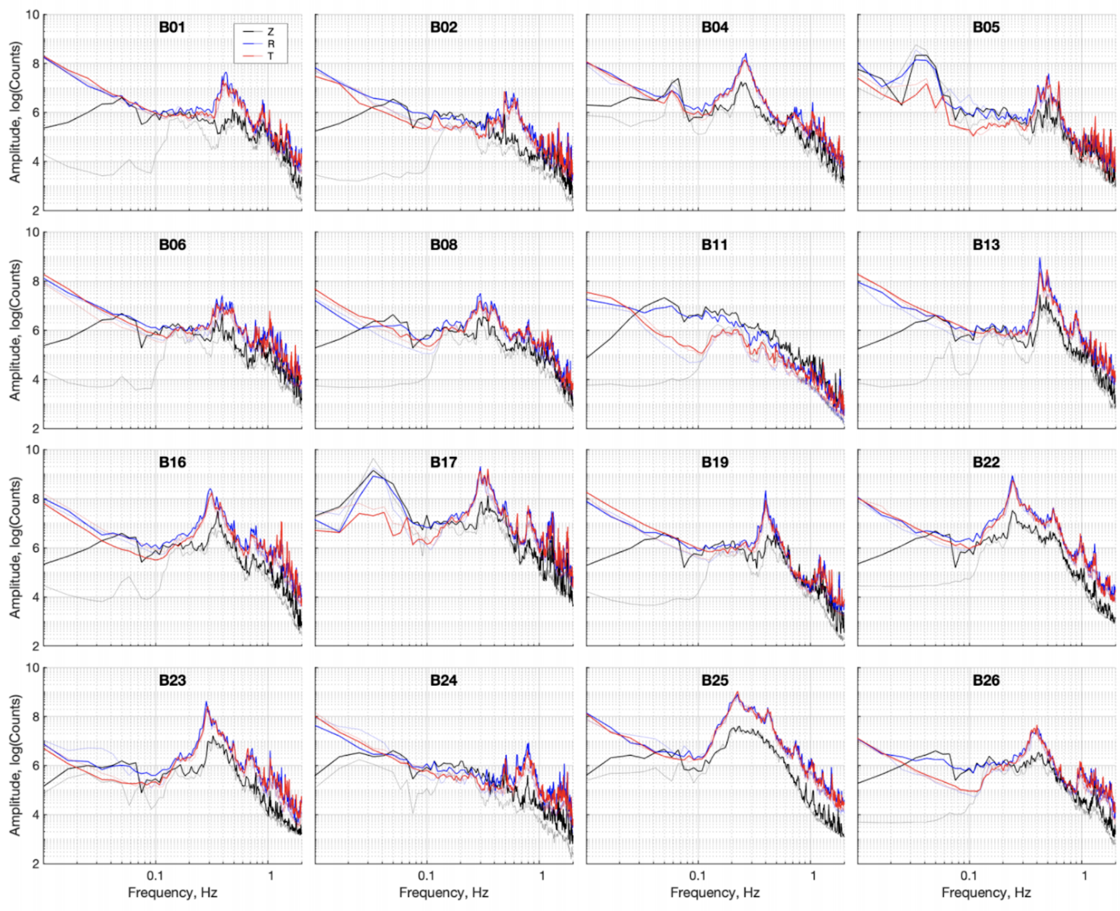


**Figure S1**. Mean power spectra for all events used at each station in this study. Black, blue and red lines indicate vertical, radial and transverse components, respectively; solid colors and lighter colors indicate P wave signal and pre-event noise, respectively. The spectra of P wave signal was calculated for a 120 s long time window starting 20 s before the P wave arrival; the spectra of pre-event noise was calculated for a 120 s long time window starting 180 s before the P wave arrival.

**Figure S2**

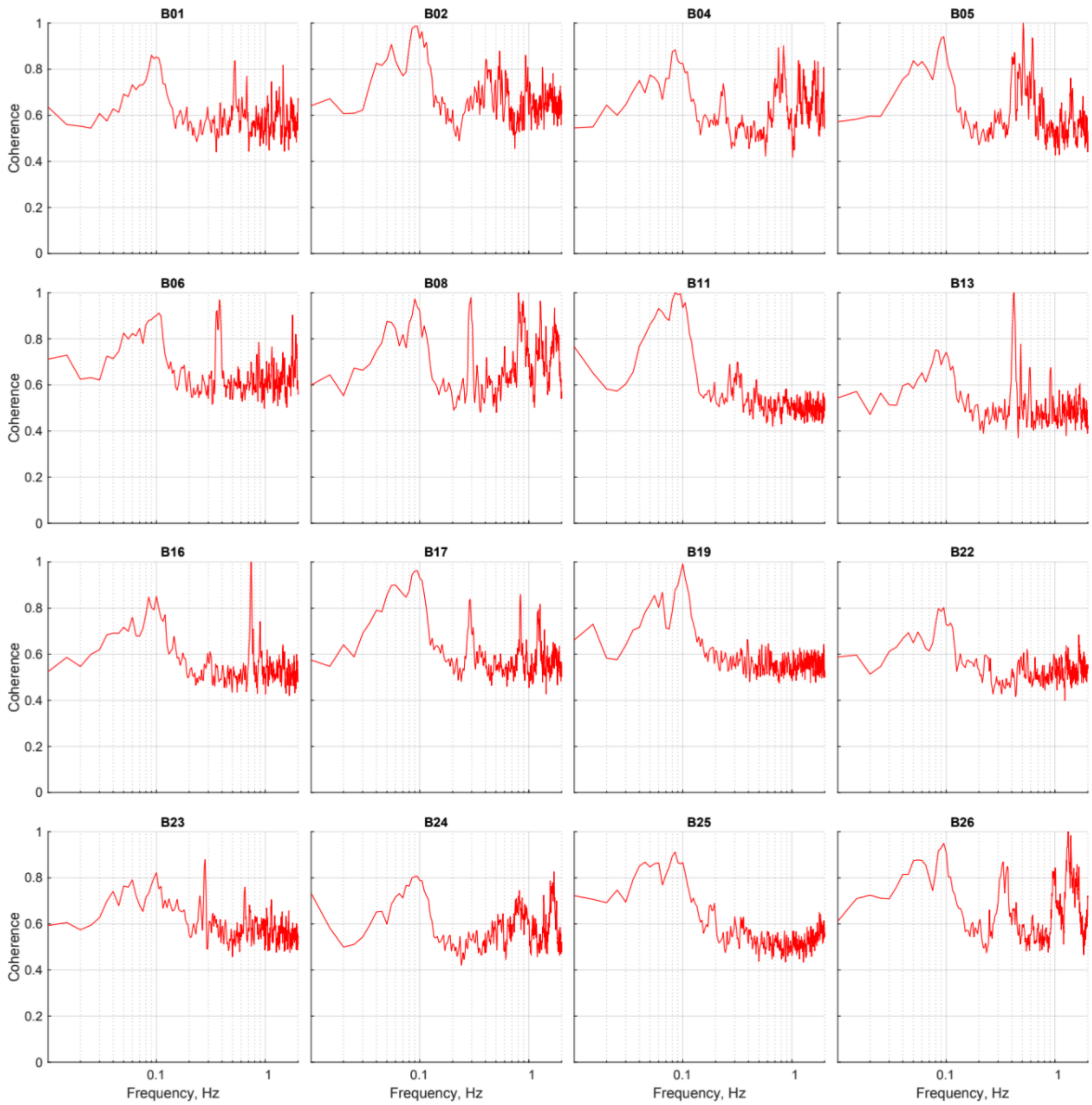


**Figure S2**. Average coherence between vertical (Z) and radial (R) components of all events used at each station.

**TABLE**

**Table S1.** Station information.

| Station | Event No. | Latitude | Longitude | Elev. (m) | $H_{Sed}$ (m) |
|---|---|---|---|---|---|
| B01 | 49 | 10.67°N | 147.50°W | -5331.5 | 209.0 |
| B02 | 52 | 11.06°N | 145.71°W | -5276.5 | 102.0 |
| B04 | 49 | 10.46°N | 146.37°W | -5111.5 | 202.0 |
| B05 | 42 | 10.78°N | 144.85°W | -5196.5 | 178.0 |
| B06 | 42 | 9.71°N | 147.75°W | -5253.5 | 279.0 |
| B08 | 46 | 8.75°N | 148.00°W | -5198.5 | 303.0 |
| B11 | 50 | 9.16°N | 146.00°W | -4889.5 | 245.0 |
| B13 | 46 | 9.25°N | 145.55°W | -5174.5 | 239.0 |
| B16 | 48 | 9.39°N | 144.88°W | -5077.5 | 228.0 |
| B17 | 38 | 9.43°N | 144.65°W | -5137.5 | 224.0 |
| B19 | 41 | 9.65°N | 143.55°W | -5058.5 | 195.0 |
| B22 | 38 | 7.81°N | 145.80°W | -5220.5 | 277.0 |
| B23 | 40 | 8.14°N | 144.29°W | -5115.5 | 258.0 |
| B24 | 40 | 8.88°N | 142.91°W | -5157.5 | 218.0 |
| B25 | 40 | 7.16°N | 146.72°W | -5109.5 | 304.0 |
| B26 | 42 | 7.54°N | 144.95°W | -5042.5 | 278.0 |

*Event No. is the number of events used in RF calculation at each station; data of $H_{Sed}$, i.e. sediment thicknesses, comes from the GlobSed model (Straume et al., 2019).